Valence Control, Reactivity of Oxygen, and Catalytic Activity of $La_{2-x}Sr_xCoO_4$

Taihei Nitadori,*,† Motohiko Muramatsu,† and Makoto Misono*,‡

Tobacco Science Research Laboratory, Japan Tobacco Inc., Umegaoka, Midori-ku, Yokohama, Kanagawa 227, Japan, and Department of Synthetic Chemistry, Faculty of Engineering, The University of Tokyo, Hongo, Bunkyo-ku, Tokyo 113, Japan

Received August 12, 1988

A series of $La_{2-x}Sr_xCoO_4$ catalysts (x = 0–2.0), which have the K_2NiF_4 structure except for x = 2.0, was prepared, and the oxidation states and compositions of both bulk and surface, as well as several properties relating to the reactivity of oxygen, were investigated. We also measured their catalytic activities for propane oxidation and found a good correlation with the oxidizing ability of the catalyst surface. The average oxidation number of Co ion monotonically increased with Sr substitution, and the composition changed from having an oxygen excess to being oxygen deficient. The composition and the oxidation state of Co ion on the surface generally agreed with those in the bulk as judged from X-ray photoelectron spectroscopy. On the basis of the reactivity and nonstoichiometry, the catalysts were divided into two distinct groups: (1) $0 \le x < 0.8$ and (2) $0.8 \le x \le 1.5$. For group 1, the desorption of the excess oxygen was observed in temperature-programmed desorption, and the amount decreased with increasing x. In group 2, the lattice oxygen desorbed, forming oxygen vacancies. The amount of oxygen desorbed, as well as the rate of isotopic exchange of oxygen, increased with x.

Introduction

The K_2NiF_4-type mixed-metal oxide (A_2BO_4) consists of alternating layers of ABO_3 perovskite and AO rock salt, being a kind of two-dimensional analogue of perovskite.[1] It is possible to change the A- or B-site ion variously without affecting the fundamental structure,[2] as in the case of perovskite-type mixed oxides.[3] Owing to this feature, the oxidation state of the B-site ion can be controlled by appropriate substitution of constituent metal elements. Therefore, the materials are suitable for the solid-state chemical study of the catalytic properties of mixed oxides.

We have previously reported the effects of Sr, Ce, and Hf substitution on the catalytic properties of perovskites, $LaBO_3$ (B = Co, Mn, Fe), and found very high activities for oxidation of hydrocarbons, which were comparable with or higher than a Pt catalyst.[4-8] Recently, we also investigated the $La_{2-x}Sr_xNiO_4$ system.[9] The valence control of $LaCoO_3$ has also been reported by Voorhoeve et al.[3] and Yamazoe et al.,[10] but the explanations for the activity changes are different. Furthermore, we noted that the effects of Sr substitution were considerably different among the Co, Mn, and Ni systems.[8,9] Therefore, we concluded that further investigations are necessary regarding the valence control of B-site ion over a wider range and its effects on catalytic properties.

In the present paper we attempt to elucidate the above relationships for a series of $La_{2-x}Sr_xCoO_4$ catalysts, for which our preliminary work indicated a good correlation between the catalytic activity for oxidation and the oxidizing power of the catalysts.[11] We measured several properties related to the reactivity of the oxygen in the catalysts, such as temperature-programmed desorption (TPD) of oxygen, the rate of isotopic exchange of oxygen, and the reducibility. We also examined the composition and the oxidation state of the Co ion on the surface by XPS. The relationships between the catalytic activity for oxidation and the properties mentioned above are discussed in the context of these results.

Experimental Section

Preparation of $La_{2-x}Sr_xCoO_4$. $La_{2-x}Sr_xCoO_4$ (x = 0–2.0) catalysts were prepared from mixtures of acetates of the metal components. The actual compositions of these mixed oxides are nonstoichiometric in general, $La_{2-x}Sr_xCoO_{4+\delta}$, but the stoichiometric formulas will be used in this paper unless explicit presentation is necessary. The mixed acetate solution was evaporated to dryness, and then the solid obtained was decomposed. It was finally calcined in a quartz crucible in nitrogen (x = 0–0.5) or in air (x = 0.8–2.0) at 1000 °C for 10 h.

Powder X-ray diffraction patterns were recorded on an X-ray diffractometer. Surface area of the samples was measured by the BET method.

The oxidation number of the cobalt ion in the catalysts was measured by iodometry. A sample (ca. 100 mg) that was dried at 100 °C for 3 h was dissolved in 25 mL of 0.4 N HCl plus 25 mL of 0.16 N KI. The solution was titrated with a standard thiosulfate solution. This method has been used for the measurement of excess oxygen in nickel oxide[12] and for the measurement of the average oxidation number of Co or Ni ion in mixed oxides.[13] The oxidation number of Co (or the nonstoichiometry) determined by this method[6] generally agreed with that obtained by using gravimetry,[14] in the case of similarly prepared $La_{1-x}Sr_xCoO_3$.

The composition of metal ions was determined with the aid of an inductively coupled plasma spectrometer (ICP). X-ray photoelectron spectra (XPS) were obtained with a Shimadzu ESCA-750 employing Mg Kα radiation (1253.6 eV) under a high vacuum of 10^{-6} Pa. The binding energy was calibrated by using a C(1s) electron line (285.0 eV) coming from the background.

Procedure. Temperature-Programmed Desorption (TPD) of Oxygen. TPD of oxygen was carried out with a flow system

* To whom correspondence should be addressed.
† Japan Tobacco Inc.
‡ The University of Tokyo.

(1) Balz, D.; Plieth, K. *Z. Elektrochem.* **1955**, *59*, 545. Galasso, F.; Darby, W. *J. Phys. Chem.* **1962**, *66*, 1318.
(2) Ganguly, P.; Rao, C. N. R. *J. Solid State Chem.* **1984**, *53*, 193.
(3) Voorhoeve, R. J. H. In *Advanced Materials in Catalysis*; Burton, J. J., Garten, R. L., Eds.; Academic Press: New York, 1977; p 129.
(4) Nakamura, T.; Misono, M.; Uchijima, T.; Yoneda, Y. *Nippon Kagaku Kaishi* **1980**, 1679.
(5) Nakamura, T.; Misono, M.; Yoneda, Y. *Bull. Chem. Soc. Jpn.* **1982**, *55*, 394.
(6) Nakamura, T.; Misono, M.; Yoneda, Y. *J. Catal.* **1983**, *83*, 151; *Chem. Lett.* **1981**, 1589.
(7) Nitadori, T.; Misono, M. *J. Catal.* **1985**, *93*, 459.
(8) Nitadori, T.; Kurihara, S.; Misono, M. *J. Catal.* **1986**, *98*, 221.
(9) Nitadori, T.; Misono, M. *Bull. Chem. Soc. Jpn.* **1988**, *61*, 3831.
(10) Teraoka, Y.; Yoshimatsu, M.; Yamazoe, N.; Seiyama, T. *Shokubai* **1984**, *26*, 106. Teraoka, Y.; Yamazoe, N.; Seiyama, T. *Hyomen Kagaku* **1988**, *9*, 153.
(11) Nitadori, T.; Misono, M. *Chem. Lett.* **1986**, 1255.
(12) Weller, S. W.; Voltz, S. E. *J. Am. Chem. Soc.* **1954**, *76*, 4695.
(13) Gushee, B. E.; Kaz, L.; Ward, R. *J. Am. Chem. Soc.* **1957**, *79*, 5601.
(14) Mizusaki, J.; Yamauchi, S.; Fueki, K.; Ishikawa, M.; Yoshihiro, M. *Annu. Rep. Eng. Res. Inst., Fac. Eng. Univ. Tokyo* **1983**, *42*, 155.

0897-4756/89/2801-0215$01.50/0 © 1989 American Chemical Society

Table I. Surface Areas, Structures, and Compositions of $La_{2-x}Sr_xCoO_{4+\delta}$ Catalysts

x^a	surface area, m^2/g	structure	δ	av ox. no. of Co ion
0	1.0	K_2NiF_4-type	0.14	2.28
0.5	1.3	K_2NiF_4-type	0.04	2.58
0.8	1.7	K_2NiF_4-type	0.03	2.87
1.0	2.6	K_2NiF_4-type	0.00	3.01
1.2	1.9	K_2NiF_4-type	0.00	3.21
1.5	2.0	K_2NiF_4-type	−0.08	3.34
2.0	1.5	unknown phase	−0.32	3.36

[a] x = 0–0.5 calcined in N_2, x = 0.8–2.0 calcined in air.

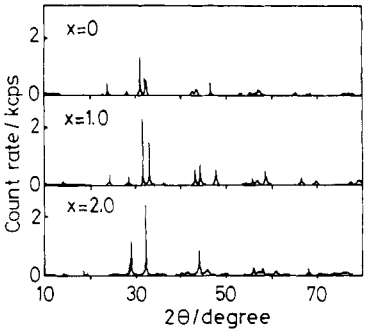

Figure 1. XRD patterns of $La_{2-x}Sr_xCoO_4$ (x = 0, 1.0, and 2.0).

using helium as a carrier gas.[4-6] Prior to each run, the sample (1.0 g) was pretreated in an O_2 stream for 1 h at 800 °C and cooled to room temperature. Then, O_2 was replaced by He at room temperature. The oxygen impurity in the He carrier gas was removed by a molecular sieve (MS) 5A trap kept at liquid nitrogen temperature. The temperature of the sample was raised at a constant rate of 20 °C min^{-1} in the He stream (25 cm^3 min^{-1}), and the oxygen desorbed was detected with a thermal conductivity detector. It was confirmed by gas chromatography that only oxygen and helium were present in the eluent gas. TPD curves were reproducible in the repeated runs after the same pretreatments.

Reduction of Catalysts by CO. The reduction of the catalysts by CO was conducted in a pulse reactor.[4-6] Prior to the reaction, the catalysts (50 mg) were treated in an O_2 stream (20 cm^3 min^{-1}) for 1 h at 300 °C, and then the O_2 stream was replaced by a He stream purified by an MS-5A trap kept at liquid N_2 temperature. The flow rate of the carrier gas (He) was 25 cm^3 min^{-1}, and the size of each pulse was 0.1 cm^3. The products were analyzed by gas chromatography.

Isotopic Exchange and Equilibration of Oxygen. ^{18}O exchange between O_2 in the gas phase and oxygen in the catalyst (denoted as "exchange" in this paper) and isotopic equilibration of O_2 in the gas phase (denoted as "equilibration") were conducted in a closed-circulation system.[4-6] Prior to the reaction, the sample (300 mg) was treated with pure O_2 (100 Torr) at 300 °C (with a trap kept at liquid nitrogen temperature) and subsequently evacuated for 1 h at 300 °C. O_2 enriched in $^{18}O_2$ (60–80%) was prepared by mixing $^{18}O_2$ (99.5%) with pure $^{16}O_2$. The isotopic composition of O_2 in the gas phase was analyzed by a mass spectrometer using intermittent sampling.

Oxidation of Propane. The catalytic oxidation of propane was carried out with a flow system.[4-6] Prior to each reaction, the catalysts (300 mg) were treated in an O_2 stream for 1 h at 300 °C. A gas mixture of propane (0.83%), O_2 (33.3%), and N_2 (balance) was the feed gas. The flow rate of the mixed gas was 60 cm^3 min^{-1}. The products were analyzed by gas chromatography.

Results

Catalysts and Their Physical Properties. The surface area, the crystal structure, and the composition of the catalysts, $La_{2-x}Sr_xCoO_4$, are summarized in Table I. The XRD patterns of x = 0, 1.0, and 2.0 samples are shown in Figure 1. The K_2NiF_4-type structure of the catalysts was confirmed by reference to the literature.[15,16] The orthorhombic structure of La_2CoO_4 changed to tetragonal upon Sr substitution for x = 0.5–1.5. The lattice constants all decreased significantly for x = 0.5 (a = 5.55, b = 5.49, and c = 12.64 Å for x = 0 and a = 5.43 and c = 12.55 Å for x = 0.5), in agreement with the previous results,[2] and then slightly decreased upon further Sr substitution. In the range x = 0–1.5, $La_{2-x}Sr_xCoO_4$ (calcined *in nitrogen* for x = 0–0.5 and *in air* for x = 0.8–1.5) had the K_2NiF_4-type structure. However, in the case of the calcination *in air* for x = 0 and 0.5, small amounts of the component oxides were formed together with the K_2NiF_4-type structure for x = 0.5, and the K_2NiF_4-type structure was not formed for x = 0. The sample with x = 2.0 showed an unknown phase. Sr_2CoO_4 with the K_2NiF_4-type structure could not be synthesized even by calcination in O_2 at 1200 °C.

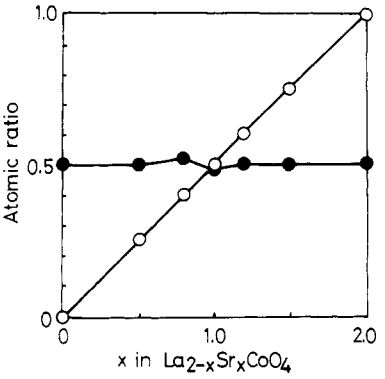

Figure 2. Composition of metallic elements in the bulk: ○, Sr/(La + Sr); ●, Co/(La + Sr).

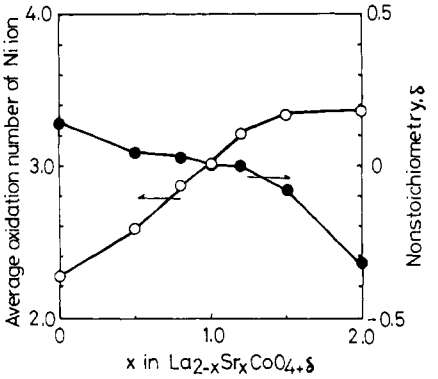

Figure 3. Average oxidation number of Co ion and the nonstoichiometry (δ) of $La_{2-x}Sr_xCoO_{4+\delta}$.

The bulk compositions of metal ions measured by ICP are shown in Figure 2. The bulk composition well agreed with the composition expected from the quantities of starting materials used.

Figure 3 shows the average oxidation number of cobalt ion at the B site measured by iodometry. The nonstoichiometry (δ in $La_{2-x}Sr_xCoO_{4+\delta}$) is also shown in Figure 3, which was calculated from the average oxidation number of cobalt ion and the valences of La, Sr, and O, which were assumed to be +3, +2, and −2, respectively. The average oxidation number of the cobalt ion monotonically increased from 2.28 (x = 0) to 3.36 (x = 2.0) with increasing x, and the nonstoichiometry varied from being oxygen-excess for x = 0–0.8 to oxygen deficient for $x \geq 1.5$. The catalysts were almost stoichiometric with respect to oxygen for x = 1.0–1.2. When the fractions of Co^{2+}, Co^{3+}, and Co^{4+} were calculated from the average oxidation number on the assumption that cobalt ions were present as either a mixture

(15) Janeck, J. J.; Wirtz, G. P. *J. Am. Ceram. Soc.* **1978**, *61*, 242.
(16) Blasse, G. *J. Inorg. Nucl. Chem.* **1965**, *27*, 2683.

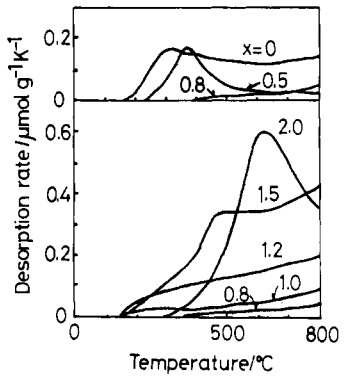

Figure 4. TPD profiles of oxygen from $La_{2-x}Sr_xCoO_4$.

Table II. Amount of Oxygen Desorption, the Corresponding Layers, and the Change of the Nonstoichiometry (See Text)

x	amt of oxygen desorbed,[a] cm^3/g	corresponding layers[b]	$\Delta\delta$[c]
0	1.76	9.8	0.06
0.5	0.73	3.1	0.02
0.8	0.19	0.8	0.01
1.0	0.50	1.6	0.02
1.2	1.58	3.4	0.05
1.5	3.48	9.2	0.10
2.0	3.46	12.8	0.09

[a] The amount of oxygen in TPD desorbed up to 800 °C. [b] The surface layers corresponding to the amounts of desorbed oxygen (assuming that the amount of oxygen in the surface monolayer was 0.96×10^{19} atom/m^2). [c] The change of the nonstoichiometry owing to the oxygen desorption ($\Delta\delta$: $La_{2-x}Sr_xCoO_{4+\delta-\Delta\delta}$).

of Co^{2+} and Co^{3+} or a mixture of Co^{3+} and Co^{4+}, the fraction of Co^{3+} showed a maximum (99%) for $x = 0$. Here, Co^{4+} is a formal expression, and this could be a positive hole on oxygen.

TPD of Oxygen. Figure 4 shows the TPD profiles of oxygen from the catalysts, where the rate of desorption is plotted against the catalyst temperature. As shown in this figure, the amount of oxygen desorbed below 800 °C decreased first with the increase in the Sr content and then increased again, showing a minimum at $x = 0.8$. The TPD profile for $x = 2.0$ was quite different. In the case of $x = 0$, slight structural changes were observed by XRD after the O_2 pretreatment at 800 °C (line broadening and appearance of weak lines of oxides of component metals).

The amounts of oxygen that desorbed below 800 °C are shown in Table II. In this table the amounts are also expressed in the unit of "surface layer" and by the change of the nonstoichiometry corresponding to the oxygen desorption. The former is the ratio of the amount of oxygen desorbed to the amount of oxygen in the surface monolayer, where the surface density of oxygen was assumed to be 0.96×10^{19} atom m^{-2}. The amount in the unit of surface layer exceeds unity, when desorption of lattice oxygen from the catalyst bulk takes place. This was the case except for $x = 0.8$. The amount of desorbed oxygen in these three units all showed minimums at $x = 0.8$. The catalyst with $x = 0.8$ (slight oxygen excess) appeared to be least sensitive to the atmosphere or the temperature.

Reduction of the Catalyst by CO (Oxidizing Power of the Surface). Figure 5 shows the results of reduction of $La_{2-x}Sr_xCoO_4$ by a CO pulse at 300 °C, which was carried out to obtain a measure of the oxidizing power of the catalyst. The ordinate indicates the percent conversions of CO to CO_2 for repeated pulses. The abscissa is the sum of CO_2 formed from the pulse and the preceding pulses and expresses the extent of the reduction of catalysts at each

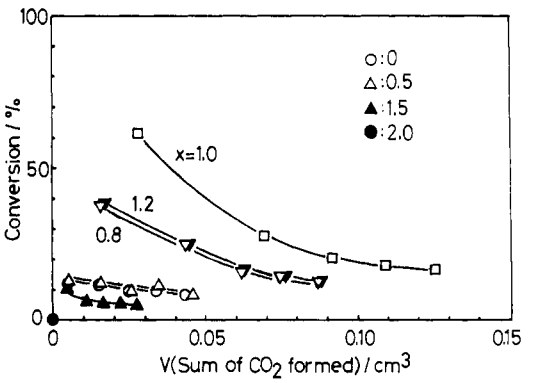

Figure 5. Reduction of $La_{2-x}Sr_xCoO_4$ by CO pulse at 300 °C.

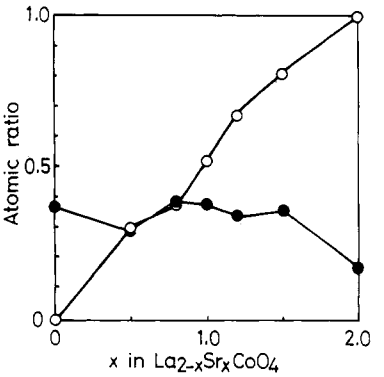

Figure 6. Surface composition of metallic elements determined by XPS: ○, Sr/(La + Sr); ●, Co/(La + Sr).

pulse. Figure 5 indicates that the reducibility of $La_{2-x}Sr_xCoO_4$ increased initially with x, but it showed a maximum at $x = 1.0$. The amount of CO_2 formed for the first pulse corresponded to 1.2 surface monolayers of oxygen at $x = 1.0$ and was less for the others. Therefore, the percent conversion of the first CO pulse reflects the reducibility at the vicinity of the surface. Hence, it may be regarded as the oxidizing power of the catalyst surface.

Surface Composition of the Catalyst. The surface compositions of the catalysts were measured by XPS as shown in Figure 6, where eq 1[17] was used for the calculations:

$$N_a/N_b = (n_a/n_b)(\sigma_a/\sigma_b)(\lambda_a/\lambda_b)(S_a/S_b) \qquad (1)$$

where N is the peak intensity, n is the atoms per unit volume, λ is the mean free path of electron, σ is the ionization cross section, and S is the instrumental factor. The peak areas of La(4d), Sr(3d), and Co(3p), including the satellite peaks, were used for N, while the values of σ were taken from the literature.[18] $\lambda \cdot S$ was assumed to be constant as in the previous work.[19] The surface compositions determined by eq 1 are not very accurate but may be sufficiently reliable to compare the relative change in the surface composition for a series of catalysts. As seen from this figure, the atomic ratio of Sr in the A site increased monotonically with x. Although the atomic ratio of Co ion was lower on the surface than in the bulk, their differences among the catalysts were not great (0.31–0.39) in the range $x = 0$–1.5, for which the K_2NiF_4-type structure was confirmed.

Figure 7 shows the XPS spectra of Co(2p) of $La_{2-x}Sr_xCoO_4$. The ratio of the satellite to main peak of $Co(2p_{3/2})$ (I_{sat}/I_{main}), the binding energy (BE), and the

(17) Hirooka, Y. *Hyomen Kagaku* **1986**, *7*, 231.
(18) Scofield, J. H. *J. Electron. Spectrosc. Relat. Phenom.* **1976**, *8*, 129.
(19) Nitadori, T.; Ichiki, T.; Misono, M. *Bull. Chem. Soc. Jpn.* **1988**, *61*, 621.

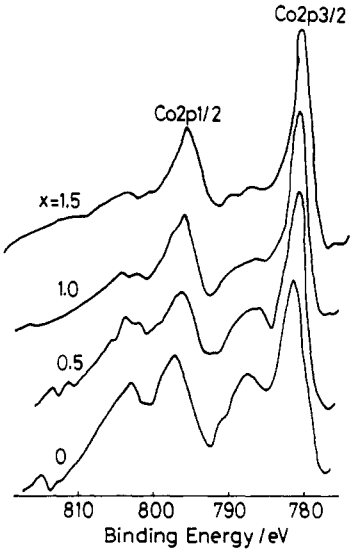

Figure 7. XPS spectra of Co(2p) in $La_{2-x}Sr_xCoO_4$.

Table III. I_{sat}/I_{main} Ratio, E Value, and Binding Energy Values of Co(2p) XPS Peaks of $La_{2-x}Sr_xCoO_4$

			BE, eV	
x	I_{sat}/I_{main}[a]	ΔE,[b] eV	$Co(2p_{1/2})$	$Co(2p_{3/2})$
0	0.44	15.6	796.9	781.3
0.5	0.42	15.6	796.3	780.7
0.8	0.31	15.3	796.1	780.8
1.0	0.30	15.3	795.9	780.6
1.2	0.27	15.1	795.8	780.7
1.5	0.22	15.2	795.6	780.4
2.0	0.24	15.4	796.2	780.8

[a] Intensity ratio of the satellite of its main peak ($Co(2p_{3/2})$). [b] Spin–orbit splitting of 2p level.

spin–orbit splitting at Co(2p) level (ΔE) are summarized in Table III. These three values generally decreased with increase in x, except for $x = 2.0$.

Isotopic Equilibration and Exchange of Oxygen. Results of the isotopic equilibration in the gas phase and the isotopic exchange between the gas and solid phase over $La_{2-x}Sr_xCoO_4$ are shown in Figure 8, where the rates of isotopic equilibration are expressed by K ($=[^{16}O^{18}O]^2/[^{16}O_2][^{18}O_2]$), which becomes 4 at equilibrium, and the rate of exchange by the extent of ^{18}O diffusion into the catalyst bulk (both at the reaction time at 90 min). The latter is represented by the number of the surface layers of the catalyst in which the ^{18}O concentration is hypothetically equal to that in the gas phase, as in our previous work.[5] The equilibration was slow at $x = 0$ and 0.5 and became faster with increase in x up to $x = 1.5$. The exchange rate decreased first and then showed a maximum at $x = 1.5$. The exchange rate was of a magnitude similar to that of the equilibration above $x = 0.8$.

Catalytic Activity for the Complete Oxidation of Propane. The catalytic activities of the catalysts for propane oxidation are shown in Table IV. The reaction products were only CO_2 and H_2O for all catalysts. As shown in this table, the oxidation activities per unit surface area of the catalysts showed a maximum at $x = 1.0$. The activation energy obtained from the data at a low conversion level below 10% was 15.1–25.0 kcal mol^{-1}.

Discussion

Structure and Composition of $La_{2-x}Sr_xCoO_4$. The previous studies[15,16,20–23] show that $La_{2-x}Sr_xCoO_4$ has a

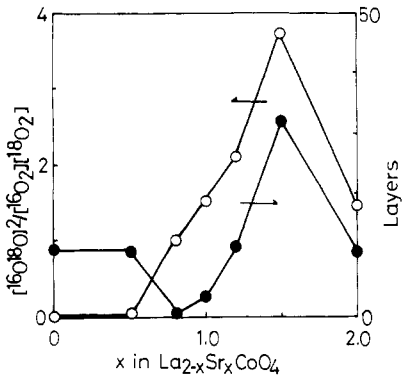

Figure 8. Isotopic exchange of oxygen over $La_{2-x}Sr_xCoO_4$: ○, equilibration; ●, exchange. See text for the ordinate.

Table IV. Catalytic Activity of $La_{2-x}Sr_xCoO_4$ for Oxidation of Propane

x	rate[a]	E_a[b]	x	rate[a]	E_a[b]
0	0.38	22.4	1.2	0.77	15.1
0.5	0.51	19.6	1.5	0.06	17.4
0.8	1.10	19.3	2.0	0.01	25.0
1.0	1.43	18.3			

[a] 10^{-2} cm^3 min^{-1} m^{-2} at 227 °C. [b] Activation energy, kcal/mol.

K_2NiF_4-type structure in the range $x = 0$–1.5 but not for $x = 2.0$, in agreement with the present study. The K_2NiF_4 structure may be unstable for Sr_2CoO_4 ($x = 2.0$) because a tetravalent oxidation state is required for all Co ions.

In the case of La_2CoO_4, since its tolerance factor is close to the lower limit of the tetragonal K_2NiF_4-type structure, the structure distorts to orthorhombic and a part of the Co ions is oxidized to trivalent, resulting in an oxygen-excess composition.[2] The composition of $La_2CoO_{4.15}$ was reported for $x = 0$ even after evacuation at 450 °C.[20] The present data are in general agreement with these previous data. The oxygen-excess composition is probably established by the formation of cation deficiencies at cation sites, as in the case of $LaMnO_3$.[24]

The valence control of the Co ion as well as the variation of the nonstoichiometry upon the Sr substitution (Table I) are similar to the case of $La_{2-x}Sr_xNiO_{4+\delta}$, in which the oxidation number of Ni ion increased from 2.32 ($x = 0$) to 2.90 ($x = 1.0$) and varied from 0.16 to −0.04.[9] The change of stoichiometry of $La_{1-x}Sr_xMnO_3$[8] was also similar. Further, the variation for $La_{1-x}Sr_xCoO_3$[6] resembled those found in the present study for $La_{2-x}Sr_xCoO_4$ above $x = 1.0$. The differences between the two Co systems are understandable, if one considers that the valence state before substitution was near +2 in the K_2NiF_4 structure and +3 in the perovskite structure.

Thus, the variations of the oxidation state and stoichiometry of these mixed oxides all appear consistent, and it may be further stated that $La_{2-x}Sr_xCoO_4$ catalysts prepared in the present study have a well-controlled oxidation state of Co and nonstoichiometry. It is noteworthy that those properties can be varied in wider range for $La_{2-x}Sr_xCoO_4$ than for $La_{1-x}Sr_xCoO_3$.

Composition and the Oxidation State of Co Ion on the Catalyst Surface. The concentration of Sr on the surface was similar to that in the bulk (Figure 6), although

(20) Matsuura, T.; Mizusaki, J.; Yamauchi, S.; Fueki, K. *Jpn. J. Appl. Phys.* **1984**, *23*, 1143.
(21) Le Coustumer, L. R.; Barbaux, Y.; Bonell, J. P.; Loriers, J.; Clerc, F. *C. R. Acad. Sci. (Paris)* **1980**, *290C*, 157.
(22) Ganguly, P.; Ramasesha, S. *Magn. Lett.* **1980**, *1*, 131.
(23) Demazeau, G.; Courbin, Ph.; Le Flem, G.; Pouchard, M.; Hagenmuller, P.; Soubeyroux, J. L.; Main, I. G.; Robin, G. A. *Nouv. J. Chim.* **1979**, *3*, 171.
(24) Tofield, B. C.; Scott, W. R. *J. Solid State Chem.* **1974**, *10*, 183.

Table V. δ Values of $La_{2-x}Sr_xCoO_{4+\delta}$ after Various Treatments

	treatment			
x	O_2, 800 °C	after TPD up to 800 °C	He, 800 °C	as prepared
0	0.43	0.37	0.23	0.14
0.5	0.10	0.08	0.04	0.04

the Co concentration on the surface was generally lower than that in the bulk. The high surface concentration of Sr for $x = 2.0$ suggests that a Sr-rich phase might have been segregated on its surface.

The electronic state of Co on the surface can be estimated by a comparison of ΔE, I_{sat}/I_{main}, and BE values with those in the literature. All of the above three parameters observed in the present study for $La_{2-x}Sr_xCoO_4$ decreased generally with an increase in x (Table III). According to the literature, BE for Co^{2+} and Co^{3+} ($2p_{3/2}$) of perovskite are 780.3 and 779.6 eV, respectively,[25] and the ΔE values of Co(2p) peaks for high-spin Co^{2+} ($t_{2g}^5e_g^2$), low-spin Co^{2+} ($t_{2g}^6e_g^1$), and diamagnetic Co^{3+} ($t_{2g}^6e_g^0$) are 16.0, 15.3–15.4, and 15.0 eV, respectively.[26] The satellite peaks are large for high-spin Co^{2+} but absent in diamagnetic Co^{3+}.[27] It was also reported for CoO and Co_2O_3 that ΔE values were 15.7 and 15.1 eV, respectively, and the satellite peak was large for CoO but very small for Co_2O_3.[28]

Hence it may be concluded from the present XPS results that Co ion on the surface became higher in oxidation state as the extent of Sr substitution increased, although there is some ambiguity for higher values of x due to the lack of information on Co^{4+} in the literature. This trend agrees with the oxidation state of Co in the bulk (Table I). The absolute BE values in the present study were higher by about 1 eV than the reported values. The differences may be due to the inaccuracy in calibration.

Effect of Sr Substitution on the Reactivity of the Oxygen of the Catalysts. On the basis of the variation of TPD profiles, the catalysts are divided into two distinct groups: (1) $0 \le x < 0.8$ and (2) $0.8 \le x \le 1.5$, except for $x = 2.0$, which had a different crystal structure. For x = 0–0.5, the large peak was observed in TPD at 300–350 °C. This is likely due to the desorption of the excess oxygen from the bulk, since the amounts were more than a surface monolayer and paralleled the amount of the excess oxygen (compare Tables I and II).

To confirm this assignment, the effects of different pretreatments on TPD and stoichiometry was examined, since the pretreatment of TPD was different from that for the measurement of nonstoichiometry. The δ values measured after several treatments were compared in Table V. The nonstoichiometry was dependent on the pretreatment, and, as expected, the treatment in O_2 enhanced the excess oxygen. However, the result is consistent with the assignment of the desorbed oxygen to the excess oxygen.

For x = 0.8–1.5, the TPD profiles were similar to each other, having no peak at 300–350 °C, and the amount of the desorbed oxygen, which was greater than a monolayer, increased with x (Table II). These behaviors as well as the changes in the valence (Co^{3+} to Co^{4+}) and nonstoichiometry (stoichiometric to oxygen deficient) are very similar to those for $La_{1-x}Sr_xCoO_3$ perovskite.[5,6] Consequently, the oxygen desorbed at a higher temperature for x = 0.8–1.5 may be ascribed to the desorption of lattice oxygen accompanying the formation of the oxygen deficiency in the bulk. Then, the valence change for x = 0.8–1.5 is considered to occur according to the following reactions:

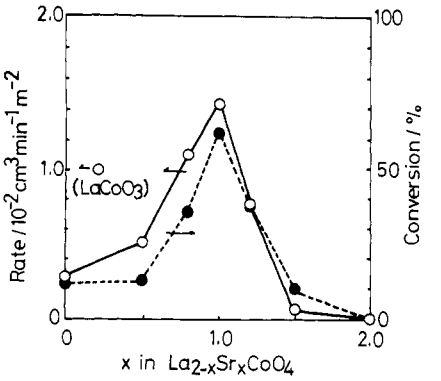

Figure 9. Rate of propane oxidation and the reducibility: ○, rate of catalytic oxidation of propane at 227 °C; ●, percent conversion of the first CO pulse at 300 °C.

$$La^{3+}{}_2Co^{2+}O_4 \xrightarrow{Sr^{2+}} La^{3+}{}_{2-x}Sr^{2+}{}_xCo^{3+}{}_{2-x}Co^{4+}{}_{x-1}O_4 \quad (2)$$

$$La_{2-x}Sr_xCo^{3+}{}_{2-x}Co^{4+}{}_{x-1}O_4 \rightarrow La_{2-x}Sr_xCo^{3+}{}_{2-x+2\delta}Co^{4+}{}_{x-1-2\delta}O_{4-\delta} + \delta/2O_2 \quad (3)$$

First, divalent Co ions are oxidized to trivalent and then to tetravalent upon Sr substitution (eq 2). With further Sr substitution, a part of unstable tetravalent Co ions tends to return to trivalent by releasing lattice oxygen (eq 3). In other words, the oxidizing ability of the catalyst increases. This is consistent with the increases in the oxygen deficiency and in the TPD peak for higher x values in this range.

The isotopic equilibration and exchange of oxygen varied in parallel with the TPD results, in the range $0.8 \le x \le 1.5$. This parallel variation was previously found for $La_{1-x}Sr_xCoO_3$.[6] Therefore, essentially the same explanation may be applied; as the composition varies from stoichiometric to oxygen deficient, the mobility of oxide ion in the bulk as well as the number of coordinatively unsaturated Co ions on the surface increases, and therefore the exchange and equilibration becomes faster. The low equilibration rate for $x \le 0.5$ (oxygen excess) may be understood by the decrease of the coordinatively unsaturated Co sites.

Effect of Sr Substitution on the Catalytic Activity for Oxidation. Although there is a report on the catalytic activity of La_2CoO_4,[21] no studies on the effect of valence control have been reported.

As is seen in Figure 9, the catalytic activity for oxidation of propane showed a maximum at $x = 1.0$. The catalytic activities of $x = 0.8$ and 1.0 are comparable with that of $LaCoO_3$.[4] This activity pattern agrees well with the variation of the oxidizing power of the surface, which is also plotted in Figure 9. The variation of the activity above $x = 0.8$ is similar to that for the $La_{1-x}Sr_xCoO_3$ system[4-6] and is also to some extent in parallel with the Co^{3+} concentration. In the case of $La_{1-x}Sr_xCoO_3$,[6] since there was no apparent correlation between the catalytic activity and the concentration of Co in any particular oxidation state, the change of catalytic activity was explained on the basis of the observed reactivity of the catalyst. That is, the activity increased upon small Sr substitution owing to the increased reactivity of oxygen, and the decrease of the activity at high extent of substitution was due to the slower reoxidation of the catalyst. Hence, the activity pattern obtained in the present study may be explained similarly

(25) Marcos, J. M.; Buitrago, R. H.; Lombardo, E. A. *J. Catal.* **1987**, *95*, 95.
(26) Frost, D. C.; McDowell, C. A.; Woolsey, I. S. *Mol. Phys.* **1974**, *27*, 1473.
(27) Briggs, D.; Gibson, V. A. *Chem. Phys. Lett.* **1974**, *25*, 493.
(28) Okamoto, Y.; Nakao, H.; Imanaka, T.; Teranishi, S. *Bull. Chem. Soc. Jpn.* **1975**, *48*, 1163.

by the reactivity of the oxide ion rather than by the concentration of Co in a particular oxidation state. In any case, we note the close correlation between the catalytic activity and the oxidizing power as shown in Figure 9. Similar correlations have been observed for $La_{1-x}Sr_xMnO_3$[8] and $La_{2-x}Sr_xNiO_4$[9] for a more limited range of x values.

Low catalytic activity for $x = 0$–0.5 (oxygen excess) is understandable, since the oxidizing power of the surface is relatively low and the ability to dissociate dioxygen is also low. The catalysts with oxygen-excess compositions showed low catalytic activities also in the cases of $La_{1-x}Sr_xMnO_3$[8] and $La_{2-x}Sr_xNiO_4$ systems.[9]

Registry No. $La_2CoO_{4.14}$, 119147-29-4; $La_{1.5}Sr_{0.5}CoO_{4.04}$, 119147-30-7; $La_{1.2}Sr_{0.8}CoO_{4.03}$, 119147-31-8; $LaSrCoO_4$, 12200-48-5; $La_{0.8}Sr_{1.2}CoO_4$, 115285-39-7; $La_{0.5}Sr_{1.5}CoO_{3.92}$, 119147-32-9; $Sr_2CoO_{3.68}$, 119147-33-0; O_2, 7782-44-7; CO, 630-08-0; Co, 7440-48-4.

Analysis of Anodic Oxide Films on Niobium

N. Magnussen,* L. Quinones, D. C. Dufner, D. L. Cocke, and E. A. Schweikert

Department of Chemistry, Texas A&M University, College Station, Texas 77843-3255

B. K. Patnaik, C. V. Barros Leite, and G. B. Baptista

Departmento de Fisica, Pontificia Universidade Catolica, Rio de Janeiro, Brazil

Received August 31, 1988

Anodic oxide films were grown on niobium in the presence of sodium tungstate. Two sample sets were grown at varying temperatures, and one set was grown to varying terminal voltages. The resulting films were examined by X-ray photoelectron spectroscopy (XPS) and Rutherford backscattering spectrometry (RBS). The XPS results show a close association of the sodium and tungstate species at the surface. Depth profiling shows the reduction of niobium oxide and the steady decrease in the amount of incorporated sodium with increased depth. The RBS data show multiple, overlapping peaks in the tungsten region. The layered structure is voltage dependent.

Introduction

Anodic oxide films are important in many applications, particularly in the area of electronic and dielectric materials. The function of the anodic film can be seriously affected by the incorporation of anions during the growth process. Recent evidence shows that the presence of foreign anions may inhibit the growth of grain boundaries and increase dielectric strength.[1,2] The incorporation of anions into anodic oxide films has been studied for several metal/metal oxide systems.[3-6] However, to date, the characterization of the niobium system has received little attention.

The surface properties of niobium are also of particular technological significance because of their impact within the field of superconducting materials. It has been determined that niobium has the highest superconducting transition temperature (9.3 K) of all the elements and also the highest transition temperature for the binary compounds, with Nb_3Ge at 23 K.[7] Of particular importance is the use of niobium for applications in superconducting ratio frequency (rf) cavities. Performance of the rf cavities is highly dependent on the surface properties of the material used. It has been suggested that anodic oxidation of the niobium surface may be one method of improving the quality of these superconducting materials.[8,9] The anodic film provides a suitable coating for the rf cavities by forming a protective, amorphous Nb_2O_5 oxide overlayer, displacing the cavity surface to a purer region within the film. Preparation techniques are critical in this matter because a few angtroms difference in oxide thickness or the presence of impurities can result in large changes in the dielectric properties and, thus, drastically affect the capabilities of the material.

The present study will consider the surface and bulk characteristics of anodic oxide films grown on a niobium substrate in the presence of tungstate anion. Tungstate was a practical choice to optimize the peak separation of the substrate (low molecular weight) and the dopant (high molecular weight) for bulk analysis in Rutherford backscattering spectrometry. The effect of temperature and voltage variations on anion incorporation will be examined through the use of X-ray photoelectron spectroscopy (XPS) and Rutherford backscattering spectrometry (RBS).

XPS is an important analytical technique for surface characterization. This technique provides information regarding the binding energies of core electrons in atoms and molecules. With this information it is possible to determine what species are at the surface and, in many cases, their oxidation state. RBS, used in the low-megaelectronvolt energy range, is a powerful technique for nondestructive depth-profiling studies. This technique can be used to determine several parameters important in the study of anodic film formation. These parameters include oxide layer thickness, stoichiometric composition, and concentration and location of the incorporated film dopants. Through the use of these two techniques, we have studied the surface and bulk characteristics of the niobium anodic oxide films, and these results are presented.

(1) Thompson, G. E.; Wood, G. C.; Shimizu, K. *Electrochim. Acta.* **1981**, *26*, 951.
(2) Shimizu, K.; Thompson, G. E.; Wood, G. C. *Thin Solid Films* **1981**, *81*, 39.
(3) Skeldon, P.; Shimizu, K.; Thompson, G. E.; Wood, G. C. *Thin Solid Films* **1985**, *123*, 127.
(4) Abd Rabbo, M. F.; Richardson, J. A.; Wood, G. C. *Corros. Sci.* **1976**, *16*, 689.
(5) Konno, H.; Kobayashi, S.; Takahashi, H.; Nagayama, M. *Electrochim. Acta.* **1980**, *25*, 1667.
(6) Sharp, D. J.; Panitz, J. K. G.; Merrill, R. M.; Haaland, D. M. *Thin Solid Films* **1984**, *111*, 227.
(7) Gavler, J. R. *Appl. Phys. Lett.* **1973**, *23*, 480.
(8) Halama, H. J. *Part. Accel.* **1977**, *2*, 335.
(9) Martens, H.; Diepers, H.; Sun, R. K. *Phys. Lett.* **1971**, *34A*, 439.

0897-4756/89/2801-0220$01.50/0 © 1989 American Chemical Society